

# Storm surge computations in estuarine and near-coastal regions: the Mersey estuary and Irish Sea area

John Eric Jones · Alan Marshall Davies

Received: 28 January 2009 / Accepted: 27 August 2009 / Published online: 26 September 2009  
© Springer-Verlag 2009

**Abstract** An unstructured grid storm surge model of the west coast of Britain, incorporating a high-resolution representation of the Mersey estuary is used to examine storm surge dynamics in the region. The focus of the study is the major surge that occurred during the period 11–14 November 1977, which has been investigated previously using uniform grid finite difference models and a finite element model of the west coast of Britain. However, none of these models included the Mersey estuary. Comparison of solutions in the eastern Irish Sea with those computed with these earlier models showed that, away from the Liverpool Bay region, the inclusion of the Mersey estuary had little effect. However, at the entrance to the Mersey, its inclusion did influence the solution. By including a detailed representation of the Mersey estuary within the model, it was possible to conduct a detailed study of storm surge propagation in the Mersey, which had never previously been performed. This detailed study showed for the first time that the surge's temporal variability within the estuary is influenced by surge elevation at its entrance. This varies with time as a function of spatial and temporal variations of wind stress over the west coast of Britain. Within the Mersey, calculations show that the spatial variability is mainly determined by changes in bottom topography, which had not been included in earlier finite difference models. However, since water depth is influenced by variations in tidal elevation, this, together with tide surge interaction through bottom friction and momentum advec-

tion, influences the surge. The ability of the finite element model to vary the mesh in near-shore regions to such an extent that it can resolve the Mersey and hence the impact of the Mersey estuary upon the Liverpool Bay circulation shows that it has distinct advantages over earlier finite difference models. In the absence of detailed measurements within the Mersey at the time of the surge, it was not possible to validate predicted surge elevations within the Mersey. However, significant insight into physical processes influencing the surge propagation down the estuary, its reflection and spatial/temporal variability could be gained.

**Keywords** Storm surge · Mersey estuary · Near-shore region · Finite element

## 1 Introduction

To date, operational storm surge prediction in the UK has focussed upon the use of shelf-wide finite difference models based upon a uniform grid. These have been complemented with locally nested limited area high-resolution models. The reason for using a shelf-wide model has been to cover a sufficiently large geographical domain to include “external surges”, which are generated in deep water and then propagate into shallower regions, e.g. the North Sea or Irish Sea. A consequence of limited computational power and the need to cover a large area is that the grid of these models has been relatively coarse [e.g. the west coast of Britain model of Davies and Jones (1992) (hereafter DJ92) used a 7-km grid]. In order to improve resolution in near-shore regions, higher resolution models [e.g. the eastern Irish Sea model of Jones and Davies (1998) (hereafter JD98) used a 1-km grid] were nested within these models. However, as shown in Davies and Hall (2002),

---

Responsible Editor: Phil Dyke

---

J. E. Jones (✉) · A. M. Davies  
Proudman Oceanographic Laboratory,  
6 Brownlow Street,  
Liverpool L3 5DA, UK  
e-mail: jej@pol.ac.uk

there can be major problems concerned with false reflection at the boundaries between these grids. In addition, the “staircase” nature of the grid in coastal regions gives rise to physically unrealistic residual flows (Davies and Jones 1996). Also with a 1-km grid, an accurate representation of the Mersey estuary is not possible.

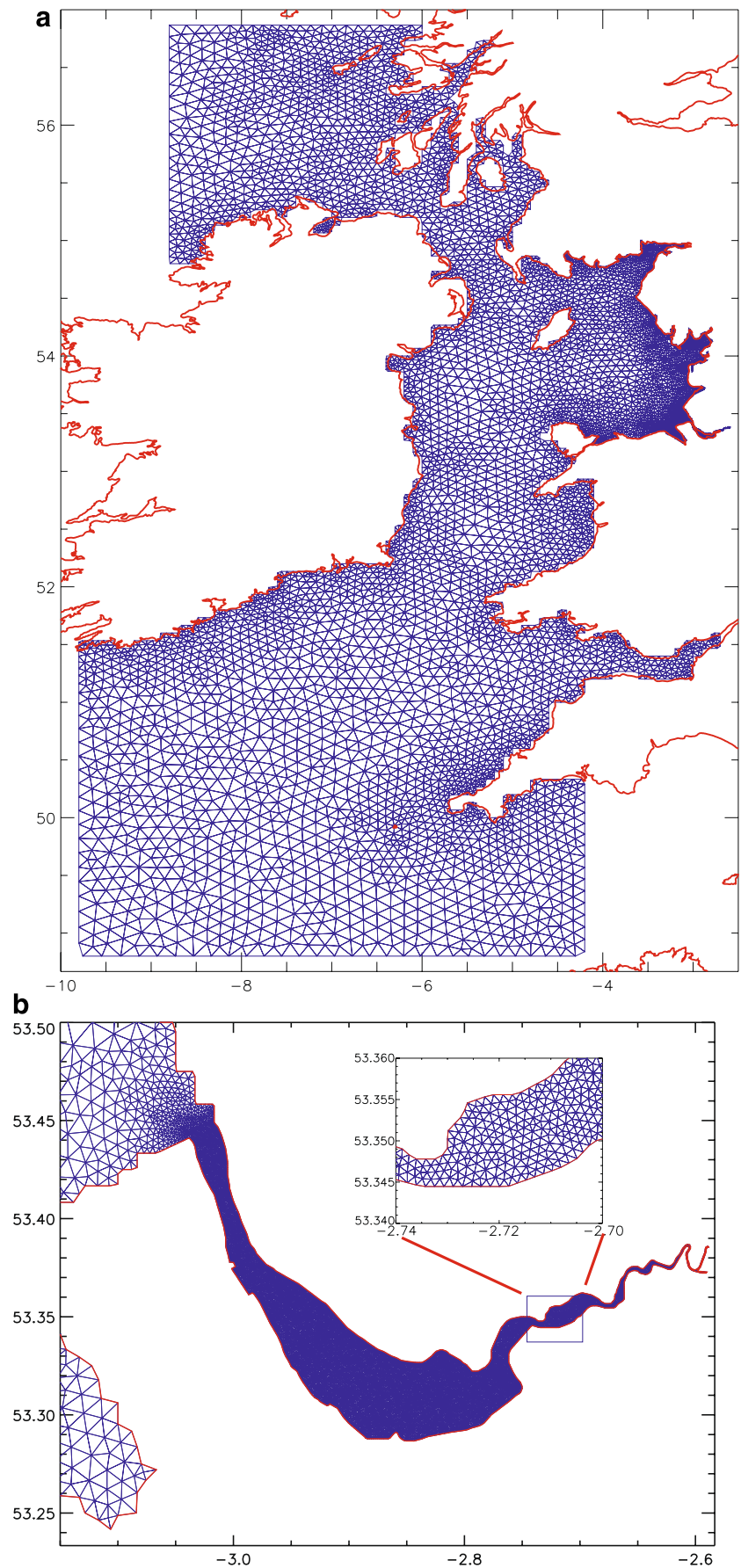
To overcome these problems, there has been significant progress in developing unstructured grids, particularly those based upon the use of finite elements. This approach with its ability to reduce the mesh size in shallow water is a valuable alternative to nesting finite difference models and has been used by a number of authors (e.g. Fernandes et al. 2002, 2004; Ip et al. 1998; Jones 2002; Lefevre et al., 2007; Nicolle and Karpytchev 2007; Walters 2005; Werner 1995). However, the choice of an optimal grid is complex (Greenberg et al. 2007; Legrand et al. 2006; 2007; Hagen et al. 2001, 2002), and in the calculations described here, no effort has been made to optimise the grid, although its size reduces as water depth decreases. Recently, Jones and Davies (2005, 2007a) showed that an unstructured grid west coastal model, based on a finite element code, namely TELEMAC, could accurately reproduce the tidal physics of the Irish Sea. The unstructured nature of the grid of the model (Fig. 1a) was such that the element size was refined in the near-shore zone. In addition, the mesh followed the coastal boundary, and the spurious eddies that occurred in tidal residuals computed with finite difference grids were not present (Jones and Davies 2007b). The major advantage of these unstructured grids was that the mesh could be progressively refined in the region of estuaries, such that a continuous solution from a large sea area to the head of an estuary could be developed. This was used to advantage by Jones and Davies (2006) (hereafter JD06) in a study of the response of the Celtic and Irish Sea regions to forcing by a uniform wind field. Subsequently, the unstructured mesh model used in these earlier calculations was further refined to include a detailed representation of the Mersey estuary (Fig. 1b), and a rigorous tidal validation of this model was performed (Jones and Davies, manuscript under (moderate) revision, hereafter JD09).

In this paper, that work is extended to the case of the storm surge of 11–14 November 1977. In addition, the finite element model of the west coast of Britain used previously (JD09), which included the Mersey estuary, that was resolved with a very fine (elements of order 50 m) unstructured grid (Fig. 1b) is applied to the present study, where the major focus is the propagation of the surge within the estuary. This surge period is particularly interesting in that the maximum surge that occurred at 0100 hours 12 November was close to the time of high water. Consequently, the likelihood of flooding was increased. In general, due to tide–surge interaction, surges

do not occur at high tide (Heaps 1983). In addition, although the surge in the Irish Sea had been studied by Jones and Davies 2008 (hereafter JD08) using a finite element model, the mesh of that model could not resolve the Mersey. In the present paper, for the first time, that region is studied in detail using a high-resolution mesh within the Mersey (see Fig. 1b and Jones and Davies, manuscript under (moderate) revision).

Initial simulations of the November surge involved a uniform 7-km grid model of the west coast covering the region shown in Fig. 2a (DJ92). Subsequently, to improve resolution in the eastern Irish Sea, the main focus of the study, resolution was refined in this area using a 1-km model nested to the west coastal model (Jones and Davies 2001). To avoid problems with nesting, in a recent study (JD08), the finite element grid given in Fig. 1a was used. Although this mesh could accurately resolve the water depth changes over the west coast of Britain (Fig. 2a) and in the eastern Irish Sea (Fig. 2b), it could not include a detailed description of the Mersey estuary (Fig. 3a), which, as shown by JD06, has an effect upon the wind forced circulation. In this paper, an extended version of that model to include the Mersey estuary, which successfully reproduced the tides in the region (Jones and Davies, manuscript under (moderate) revision), is used to study the November 1977 storm surge. The depth distribution in Liverpool Bay in the region close to the entrance to the Mersey (Fig. 3a) is characterised by a deep (depths of order 20 m) channel on its eastern side with shallower water to the west, particularly close to the northern tip of the Wirral peninsular (location A), where near-shore depths are above mean sea level (MSL) and “wetting and drying” occurs over a tidal cycle. Similarly, towards the head of the estuary and at its southern extent, water depths are above MSL and extensive areas can “wet and dry” over the tidal cycle (Fig. 3a). The numerical methods used to incorporate this “wetting and drying” into the finite element code are discussed in the next section. Near the head of the estuary, namely east of  $2^{\circ} 41' W$ , the bottom topography exhibits extensive small-scale variability (Fig. 3b). At about  $2^{\circ} 39' W$  (location W, on Fig. 3b), there is a shallow water region across the whole width of the channel, which will impede flow in it. Similar bar-type features exist farther east at locations X and Y. In addition, at Y, there is a shallow region on the southern side of the estuary. In the upper reaches of the estuary, the water is significantly shallower, with a particularly shallow water region (water depths of order 10 m above MSL) occurring at position Z (Fig. 3b). In these regions, “wetting” will only occur during a major positive surge, as water depths are above the local spring tide. In the present model, unlike in JD08, the finite element mesh has been refined in the Mersey region to such an extent that it can resolve these changes in topography (Fig. 1b).

**Fig. 1** **a** Finite element mesh of the west coast of Britain region, **b** expanded mesh in the region of the Mersey estuary with insert showing highly expanded mesh in the upper reaches



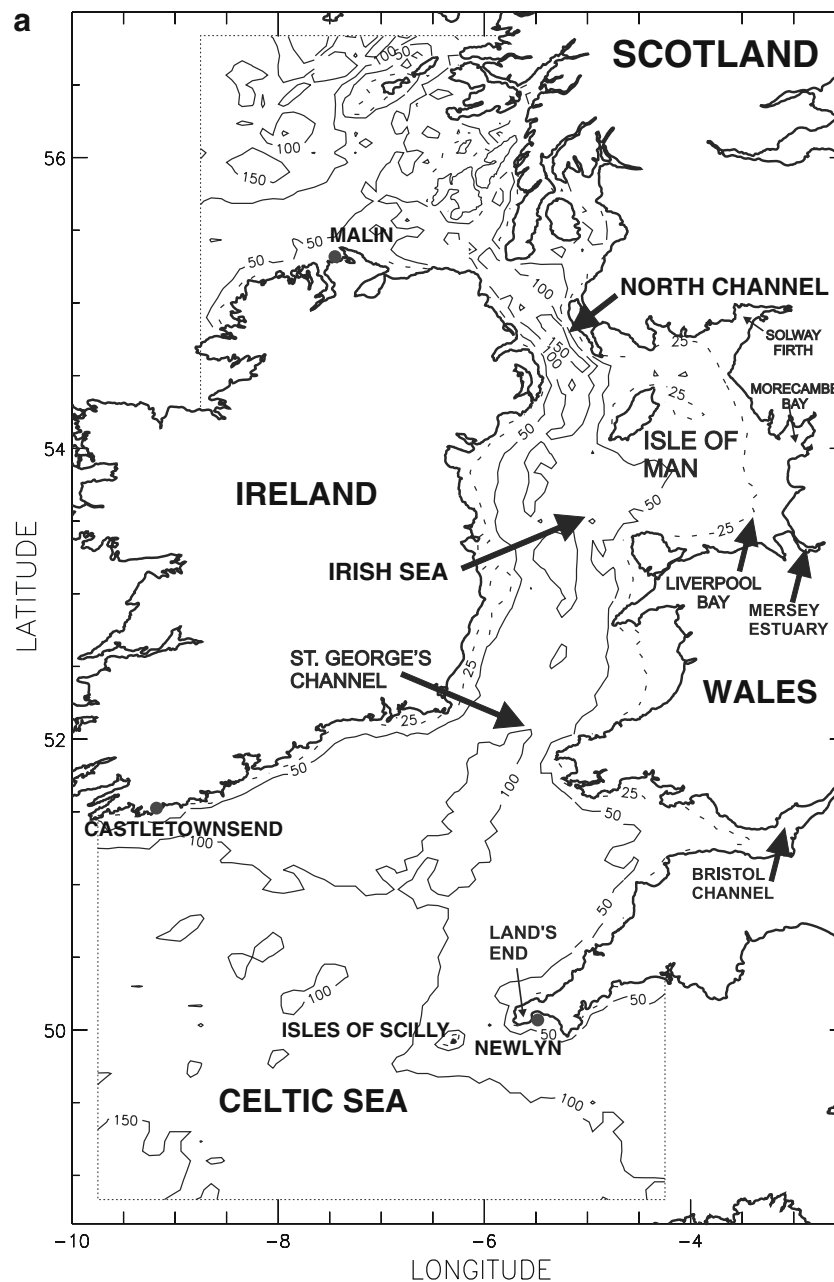


**Fig. 2** a Topography of the region covered by the model and places named in the text, b expanded sub-domain in the eastern Irish Sea

In essence, in the present paper, the finite element west coast model of JD08, is extended to include the Mersey estuary, and the propagation of the November 1977 surge in this region is examined. By this means, surge propagation along the west coast of Britain into the eastern Irish Sea and down the Mersey estuary is investigated. To the authors' knowledge, this is the first time that such a detailed study of a west coast storm surge has been performed. Details of the model are presented in the next section, with subsequent sections describing results from the storm surge simulation.

A final conclusions section presents the major findings of the work.

## 2 Storm surge finite element model

Since details of the model are given in JD06, only the main points are presented here. As in the majority of storm surge investigations, since the main emphasis is on surge elevation, then only the vertically integrated two-

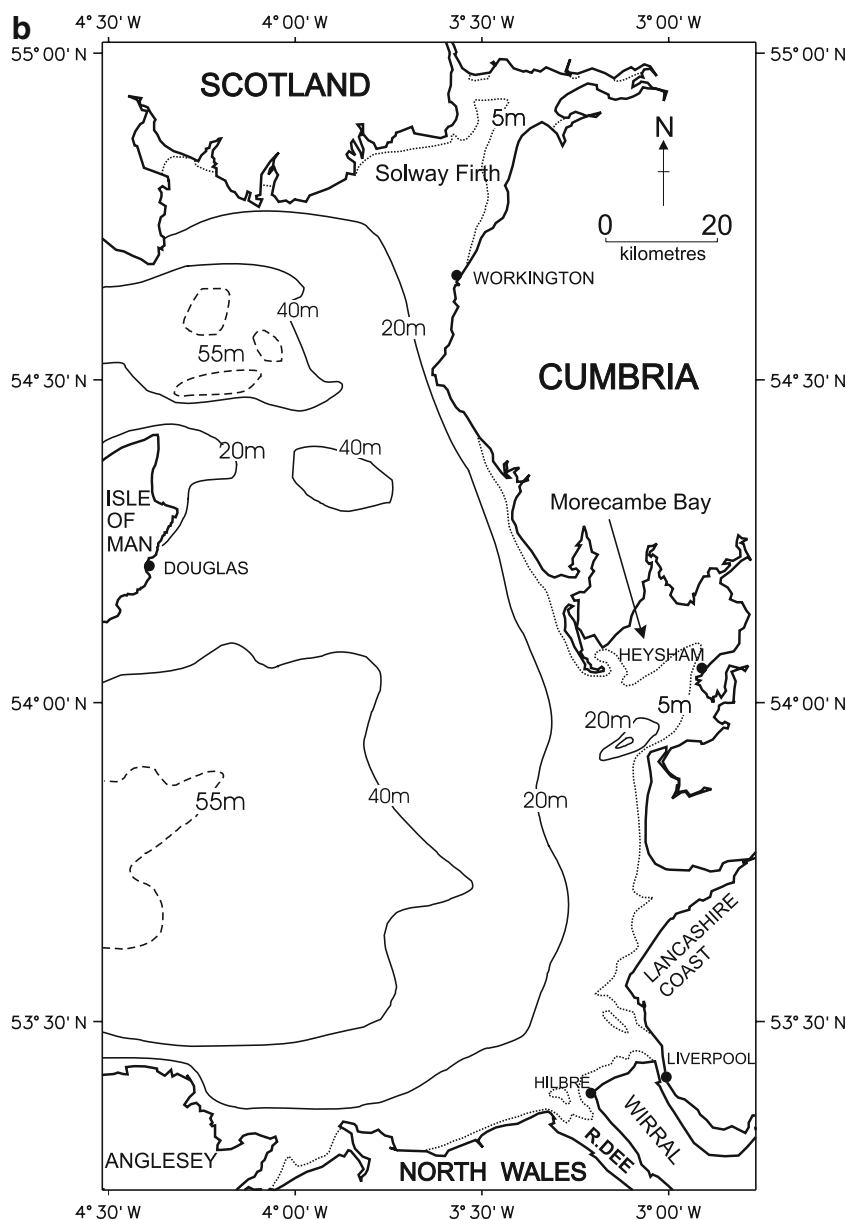
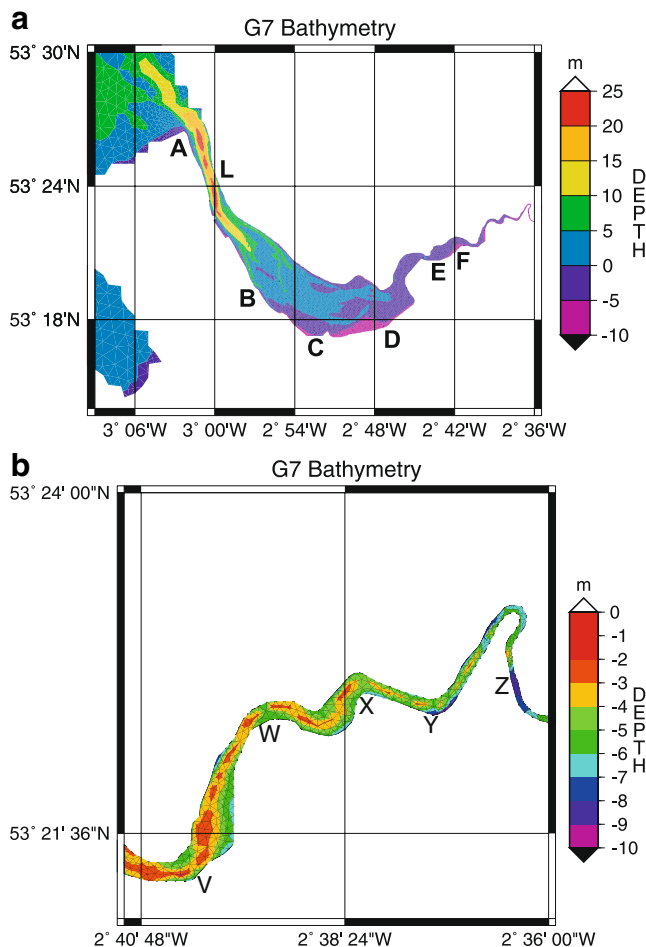


Fig. 2 (continued)

dimensional non-linear hydrodynamic equations are solved. However, since the model’s region (Fig. 1a) covers a range of latitude, the spherical coordinate form of the equations was used. As these are given in JD06 and elsewhere (e.g. DJ92, Davies et al. 1998) they will not be given here. Nevertheless, it is important to include “external surges” entering the region (see later). Bottom stress was parameterized using a quadratic friction law with drag coefficient  $k=0.0030$ . Unlike some storm surge work using small area models where the spatial variability of the wind stress is neglected, in the present calculations, the wind stress varied over the whole domain. Time and space varying surface wind stresses were identical to those used in JD08 and DJ92 for the November 1977 surge were applied at the sea

surface. As a detailed discussion of the meteorological forcing is given in DJ92, it will not be repeated here. The geographical extent of the model and water depths were identical to those used in DJ92 and JD08, with the addition of the Mersey where water depths were taken from Lane (2004). By this means, solutions could be compared with the finite difference model of DJ92 and the finite element model of JD08, which did not include the Mersey. As in DJ92, JD08 and Jones and Davies (manuscript under (moderate) revision) the five dominant tidal constituents, namely  $M_2$ ,  $S_2$ ,  $N_2$ ,  $K_1$  and  $O_1$  were included along the open boundary of the model in order to take account of tidal friction and tide–surge interaction in the region. The surge was computed by subtracting the tidal solution from





**Fig. 3** **a** Topography of the Mersey estuary with **b** expanded sub-domain near the head of the estuary. Also given are locations, indicated by letters, where specific features of the surge are discussed in the text, with *L* indicating the location of Liverpool

that involving tide and surge. However, as shown in JD06, this method in shallow water leaves some tidal energy in the computed storm surge residual. This is also found when observations are detided in this way, (e.g. Bernier and Thompson 2006; Bobanovic et al. 2005; Horsburgh and Wilson 2007) and is due to tide–surge interaction. As this method of de-tiding the surge is consistent with approaches used in earlier finite difference calculations, it is applied here. Hence, a “like with like” comparison is possible.

As shown in DJ92 and JD08, it is not just the local wind over the region that influences the storm surge but also that outside the model domain. To take account of “far field” effects in the surge calculation, an external surge elevation was included along the open boundary. This was done by linearly interpolating observed surge elevations from Castletownsend and Newlyn along the southern open boundary. Along the open northern boundary surge elevations were taken from surge observations at Malin. Although this is not ideal, it is consistent with DJ92 and

JD08, and hence, the solution from the present model can be compared with those derived previously.

Along coastal boundaries, the normal component of velocity was set to zero, with the horizontal gradient of along shore component also taken as zero, corresponding to perfect slip at the coast. In shallow coastal regions, “wetting” and “drying” can occur during the tidal cycle and also due to changes in storm surge elevation. In high-resolution finite difference models (e.g. Jones and Davies 1998), this was taken into account using the methods of Flather and Hubbert (1989). In the finite element approach, a range of options exist as discussed in Ip et al. (1998), and there are various options in the TELEMAC code. The option used here (see JD06 for details) is consistent with the approach of Flather and Hubbert (1989) and hence with earlier finite difference studies of the November 1977 surge.

### 3 Calculation of the storm surge of 10–14 November 1977

As in earlier finite difference studies (e.g. DJ92, JD98) and the calculations performed using the west coast finite element model (Fig. 1a), without the Mersey (JD08), motion was induced from a state of rest by the imposition of tidal and external surge elevation forcing along the open boundary and surface wind stress forcing. A parallel tide-only solution was obtained with just tidal forcing, and hence, the surge elevation and current were determined by subtracting this tidal solution from the total. As surge dynamics over the whole region and comparisons with earlier finite difference models are considered in JD08, the focus here will be the Liverpool Bay region and in particular the Mersey estuary. Since the Mersey was not included in JD08, its role in determining the surge (both elevations and currents) and the spatial and temporal variability of the surge in the Mersey will be considered in detail.

#### 3.1 Storm surge event of 1800 hours 10 November to 2200 hours 10 November 1977

##### 3.1.1 Surge propagation in the eastern Irish Sea and Mersey Estuary

Since details of the meteorological forcing are given in DJ92, only the major aspects will be presented here. Consider initially the build up of westerly winds over the Irish Sea (as shown by the time series at a point in the centre of Liverpool Bay, Fig. 4a) associated with a depression that moved from west to east over the region to the north of Scotland. Initially (1800 hours 10 November), there was a nearly uniform increase in sea level (positive surge of order 0.3 m) over the whole eastern Irish Sea as the

south-westerly winds drove water into the region (for details see DJ92). However, there was no appreciable surge penetration in the shallow water estuarine coastal regions of the eastern Irish Sea, namely the Solway Firth, Morecambe Bay and at the head of the Mersey and Dee estuaries. Although there was no surge build-up in the shallow water region to the north of the Wirral peninsular (Fig. 5a, location A), the surge had penetrated down the Mersey in the deep water channels as far as location B, although shallow water areas at location C and toward the head of the estuary were unaffected.

Subsequently (2000 hours 10 November), as the surge propagated northward through the eastern Irish Sea, elevations in the southern half of the region decreased [Fig. 5b, (i)]. Associated with the northward movement of the surge, water levels in the Solway estuary and Morecambe Bay increased [Fig. 5b, (i)]. Although surge levels in Liverpool Bay had decreased, the surge within the Mersey [Fig. 5b, (ii)] continued to propagate up the estuary as far as the shallow region at location C.

As the surge propagated northward in the eastern Irish Sea, surge levels within the Solway estuary and Morecambe Bay continued to rise reaching values in excess of 0.5 m near the head of these estuaries. This rapid increase arose due to wind forcing and the propagation of the surge into increasing shallow water. In the Mersey estuary at 2100 hours 10 November (Fig. 5c), despite the significant decrease in surge level at its entrance, the surge continued to propagate in the deeper water channel to the north of the shallow region at location D.

Over the next hour, surge levels at the head of the Solway estuary and Morecambe Bay continued to rise, reaching a value in excess of 1.0 m within Morecambe Bay at 2200 hours 10 November, despite the fact that, at its mouth, the surge elevation was only of the order of 0.1 m. Similarly, within the Mersey (not shown), the surge peak continued to propagate down the estuary as far as the narrow constriction at location W (Fig. 3b).

This period, namely 1800 hours 10 November to 2200 hours 10 November, clearly shows that even during the early stages of storm surge development, a propagating surge can be generated at the entrance to an estuary, with subsequent propagation down the estuary. In particular, the down estuary propagation continues with increasing storm surge elevation for sometime after the surge at the entrance to the estuary has decreased. This relationship between surge elevation at the entrance to the Mersey and surge propagation within the estuary had not been previously

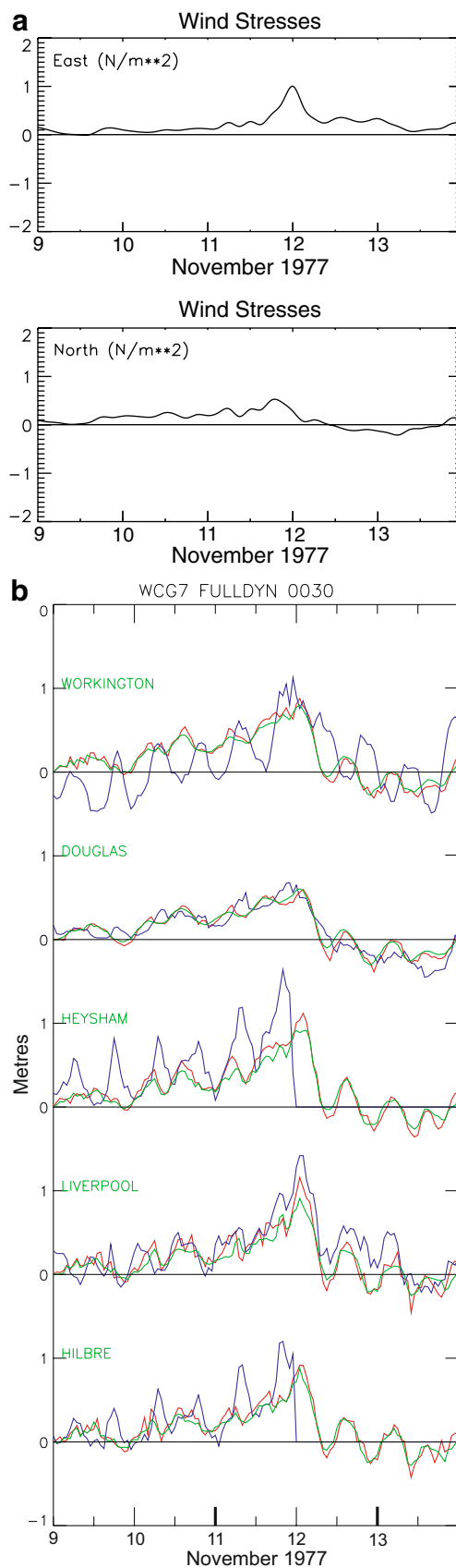


**Fig. 4** a Time series for the period 9–14 November of east and north components of wind stress in  $N\ m^{-2}$ . b Time series of storm surge elevation (m) at a number of eastern Irish Sea ports. Blue line observed, red line from Jones and Davies (1998), green line present calculation

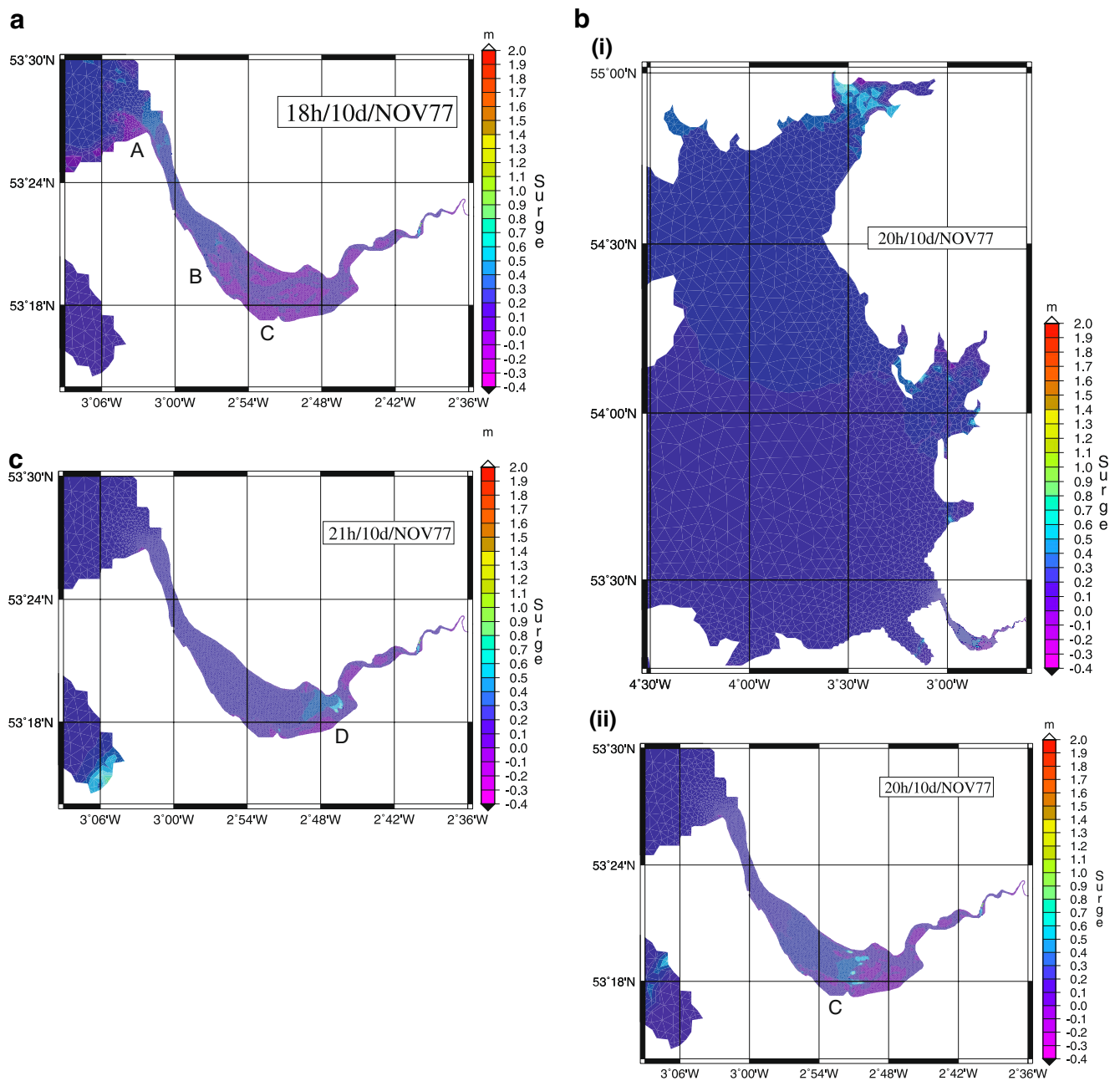


**Fig. 5** **a** Contours of computed surge elevation ( $m$ ) over the Liverpool Bay and Mersey estuary region at 1800 hours 10 November. **b.** (i) Contours of computed surge elevation ( $m$ ) over the eastern Irish Sea

and (ii) over the Liverpool Bay and Mersey estuary at 2000 hours 10 November. **c** Contours of computed surge elevation ( $m$ ) over the Liverpool Bay and Mersey estuary at 2100 hours 10 November

realised due to the coarse representation of the Mersey in previous models (JD98 and JD08).

### 3.2 Storm surge of 0600 hours 11 November to 0600 hours 12 November 1977

#### 3.2.1 Surge propagation in the eastern Irish Sea

As the large-scale features (namely the eastern Irish Sea region) of this surge have been discussed in JD98 and

JD08, only the main points will be described here, with the detailed description focusing on the Mersey, which was not included in this earlier work. The major storm surge during this period was produced by a depression that moved from west to east from the region to the north of Scotland towards northern Norway. Initially (0600 hours 11 November) as the magnitude of the south-westerly winds over the region increased, surge levels within the Irish Sea rose (see JD98 for details), although there was no initial propagation into the shallow regions at the head of the estuaries. Later



(1200 hours 11 November to 1800 hours 11 November), there were strong (wind stresses exceeding 0.5 Pa) winds from the southwest of the Celtic and Irish Seas, which subsequently changed with an increase in magnitude (stresses up to 1.5 Pa) to winds from the west (0000 hours 12 November; Fig. 4a). Over the following 12 h (up to 0012 hours 12 November), the strength of these winds declined. During this period, the west coast of Britain was subjected to significant spatially and temporally varying wind stress, characterised by winds from the southwest changing to westerly. These winds produced an increase in surge levels within the estuaries of the eastern Irish Sea, particularly the Mersey [Fig. 6a, 6b(i) and 6b(ii)] (see later discussion).

During the period of strong south-westerly winds, sea levels rose in the eastern Irish Sea [Fig. 6c, (i)], 1800 hours 11 November, with the largest rise in shallow water, particularly in the northern part of the region. This produced a northwest elevation gradient [Fig. 6c, (i)] aligned with the wind stress direction. As the wind's direction changed and its intensity increased, surge elevations in the eastern Irish Sea increased as shown in the contour plots [Fig. 6d, (i), 2300 hours 11 November] and time series at eastern Irish Sea ports (Fig. 4b). Unfortunately, there are no surge elevation time series from tide gauges within the Mersey, which were badly damaged due to the strength of the surge. A west–east surge elevation gradient, aligned with the westerly wind direction, is evident [Fig. 6d, (i)]. Subsequently, as the wind magnitude decreases, surge elevations over the eastern Irish Sea diminish with an associated decrease at individual ports (Fig. 4b). These variations in storm surge elevation in the eastern Irish Sea are not significantly different from those found in JD98, using a limited area (eastern Irish Sea) high-resolution (1-km grid) finite difference model. In addition, they are in close agreement with the solution presented in JD08 based upon a comparable model without the inclusion of the Mersey. However, as the main focus of this paper is the propagation and spatial variability of the surge in the Mersey estuary, this will be discussed in detail in the next section.

### 3.2.2 Surge propagation in the Mersey

It is evident from the time series of observed and computed storm surge elevations at west coast ports in particular at Liverpool, situated close to the entrance to the Mersey, that surge elevation starts to increase from 0000 hours 11 November (Fig. 4b), as elevations increase over the eastern Irish Sea.

Contours of surge elevations in Liverpool Bay and within the Mersey at 0600 hours on 11 November show (Fig. 6a) the surge entering the Mersey with its magnitude increasing as it propagates down the estuary. It is apparent

(Fig. 6a) that there is significant spatial variability in the surge elevation, with maximum values in Liverpool Bay and at the entrance to the Mersey occurring in the deep channel on the eastern side of the Mersey (Fig. 3a). In these regions, bottom frictional effects are less than in shallow water, and the surge amplitude is larger. As the Mersey shallows, the surge amplitude increases, although it is larger in the deeper channel than shallower regions. This is evident in the spatial distribution of the 0.5-m contour (Fig. 6a), which appears to follow the deep channel (Fig. 3a) in the Mersey entrance. However, the surge maximum increases as it propagates down the Mersey due to water depth decreasing, giving rise to a maximum in the deep water channel north of location B (Fig. 6a). It is interesting to note that, despite the increase in surge elevations within the Mersey, part of the shallow water region at the northern tip of the Wirral (location A, Fig. 6a) does not have a significant surge elevation during the period. The shallow water depths in this region inhibit the surge propagation, which mainly occurs in the deep water channel of the Mersey.

By 1200 hours 11 November, the surge maximum (of order 1.0 m) has propagated into the upper reaches of the Mersey, as far east as  $2^{\circ}40' \text{ W}$  [Fig. 6b, (i) and (ii)]. At this time, surge elevation at Liverpool has exceeded 0.4 m, and there is little spatial variability in surge elevation in the western part of the Mersey. However, in the southern part of the Mersey (south of  $53^{\circ}18' \text{ N}$ ), between  $2^{\circ}54' \text{ W}$  and  $2^{\circ}46' \text{ W}$  where there are extensive dry regions, the surge elevation is near zero [see the region close to locations C and D in Fig. 6b, (i)]. This suggests that the surge propagation within the Mersey follows the deep water channels. In shallow regions, near the head of the Mersey, the surge elevation has significantly increased [Fig. 6b, (ii)], due to shallowing of the water and the propagation of the surge in the deeper water regions from the mouth of the river.

As the surge maximum enters the upper reaches of the river, some reflection occurs. This reflected wave, together with the incoming wave, gives rise to an overall increase in water levels within the Mersey. By 18 hours 11 November (near tidal low water), surge elevations in Liverpool Bay [Fig. 6c, (i)] and at the entrance to the Mersey [Fig. 6c, (ii)] exceed 0.5 m, due to the strong south-westerly wind. It is evident [Fig. 6c, (ii)] that, in the Liverpool Bay region at the entrance to the Mersey, there is appreciably small scale variability in the surge elevation. In this area and within the Mersey, maximum elevation occurs in the deeper water. This is particularly evident at the entrance to the Mersey with little surge elevation in the region centred on  $53^{\circ}26' \text{ N}$ ,  $3^{\circ}04' \text{ W}$  [location A; Fig. 6c, (ii)], a shallow water area (Fig. 3a), whereas to the northeast of this in the deep water channel (Fig. 3a), surge elevations exceed 0.4 m. Similarly within the Mersey, the surge maximum extends as far south as position B, although the shallow water region to the

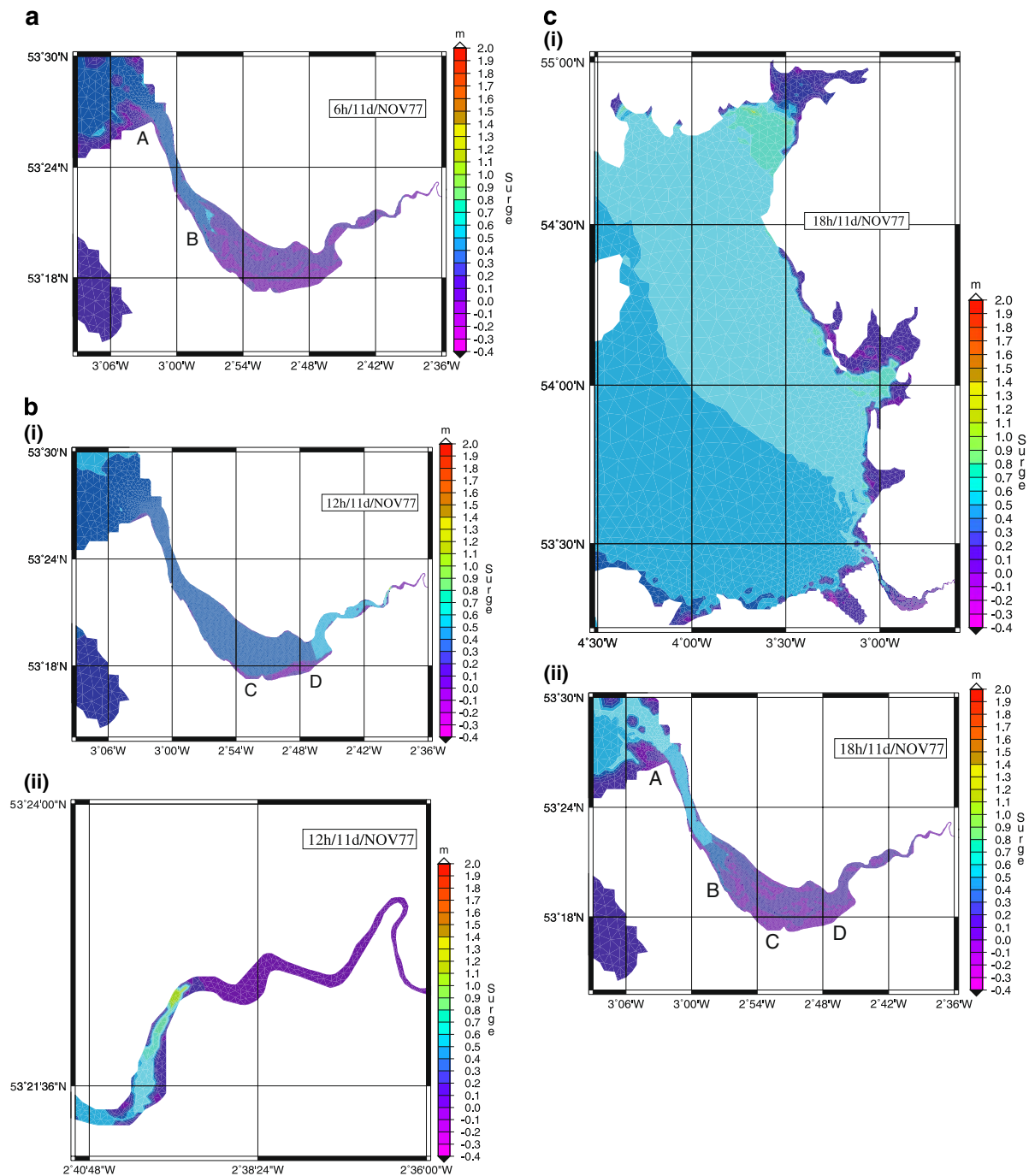


**Fig. 6** **a** Contours of computed surge elevation ( $m$ ) over the Liverpool Bay and Mersey estuary at 0600 hours 11 November. **b** **(i)** Contours of computed surge elevation ( $m$ ) over the Liverpool Bay and Mersey estuary and **(ii)** the upper reaches of the Mersey at 1200 hours 11 November. **c** **(i)** Contours of computed surge elevation ( $m$ ) over the eastern Irish Sea and **(ii)** over the Liverpool Bay and Mersey estuary at 1800 hours 11 November. **d** **(i)** Contours of computed surge elevation ( $m$ ) over the eastern Irish Sea, **(ii)** over the Liverpool Bay and Mersey estuary and **(iii)** currents within the upper reaches of the Mersey at 2300 hours 11 November. **e** **(i)** Contours of computed surge elevation ( $m$ ) over the Liverpool Bay and Mersey estuary and **(ii)** the

upper reaches of the Mersey at 0000 hours 12 November. **f** **(i)** Contours of computed surge elevation ( $m$ ) over the Liverpool Bay and Mersey estuary region, **(ii)** within the upper reaches of the Mersey and **(iii)** currents within the upper reaches of the Mersey at 0100 hours 12 November. **g** **(i)** Contours of computed surge elevation ( $m$ ) over the Liverpool Bay and Mersey estuary region, **(ii)** within the upper reaches of the Mersey at 0200 hours 12 November. **h** Contours of computed surge elevation ( $m$ ) over the Liverpool Bay and Mersey estuary region at 0300 hours 12 November. **i** Contours of computed surge elevation ( $m$ ) over the Liverpool Bay and Mersey estuary region at 1100 hours 12 November

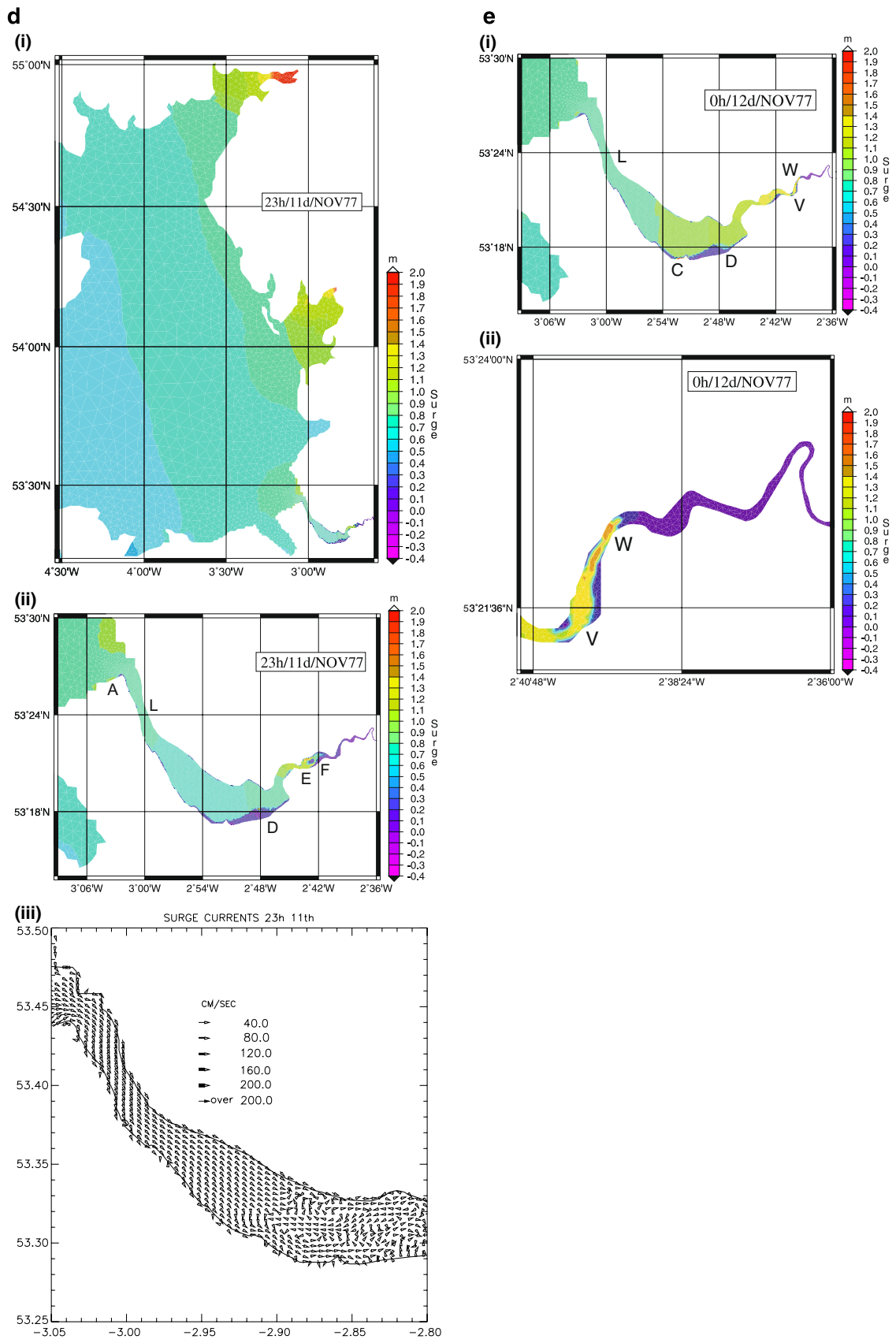


Fig. 6 (continued)

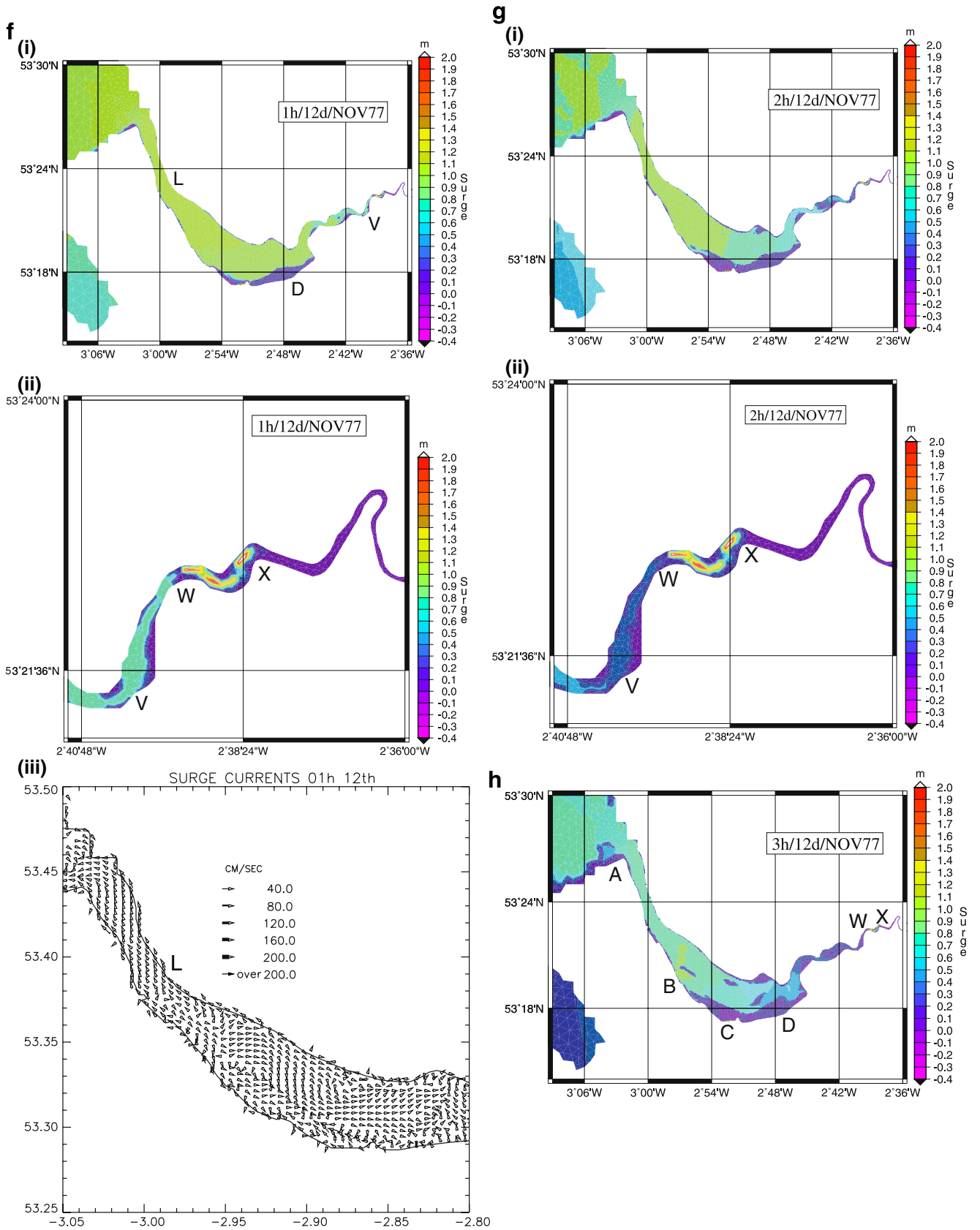


Fig. 6 (continued)

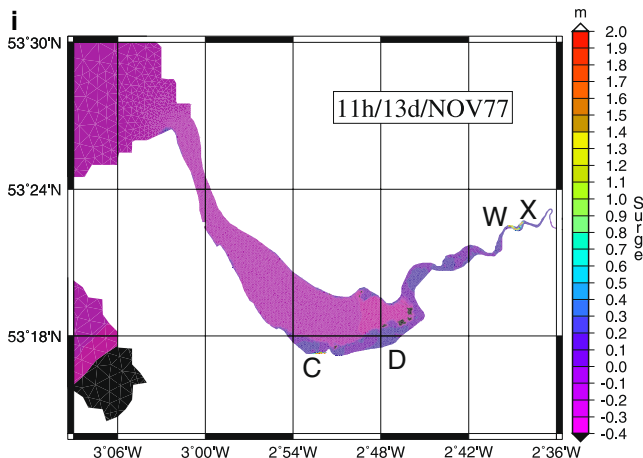


Fig. 6 (continued)

southeast of this (the region close to locations C and D) remains dry.

This surge distribution at 1800 hours 11 November [Fig. 6c(ii)] within the Mersey and at its entrance is similar to that found about 12 h earlier at 0600 hours 11 November (Fig. 6a). As shown by JD06 and found in observations, significant tide–surge interaction can occur in shallow water regions such as the Mersey that leads to a modification of the tidal amplitude. Consequently, when the tide from a tide-only calculation is used to de-tide the tide and surge calculation in order to calculate the surge, some tidal energy remains in the surge. This explains the semi-diurnal oscillations found in both the observed and computed time series (Fig. 4b) particularly at shallow water ports (e.g. Heysham, Liverpool and Hilbre) and the similarity between Fig. 6a and c (ii). In addition to tide–surge interaction modifying the semi-diurnal tide, it also has a significant effect upon the higher harmonics, giving rise to small-scale location variations in these harmonics. This small-scale variability will appear in the surge derived by de-tiding tide plus surge in shallow water and, together with local variations in water depth, explains some of the spatial variability in the surge that is evident in Fig. 6a and c (ii).

Over the next 5 h, namely from 1800 to 2300 hours on 11 November, the wind magnitude increases over the Irish Sea, with wind direction changing from south-westerly to westerly. This wind change gives rise to the maximum surge that occurred during this surge period, namely elevations exceeding 1.5 m in the northeast corner of Morecambe Bay and at the head of the Solway estuary, at 2300 hours 11 November [Fig. 6d, (i)]. Note that this is the moment of tidal high water at Liverpool. The spatial distribution of storm surge elevations over the eastern Irish Sea reveals [Fig. 6d, (i)] a significant rise in the Liverpool Bay region.

As water levels in Liverpool Bay rise, the surge in this region [Fig. 6d, (ii)] propagates farther into the estuary reaching location E [Fig. 6d, (ii)]. In this region, the cross-sectional area of the Mersey is significantly reduced leading to an intensification of surge magnitude in the region to the north of location E. Just to the east of this, surge propagation in the centre of the river is inhibited by an area of shallow water (location F). As previously [Fig. 6b, (i) and (ii)] although surge elevation within Liverpool Bay and at the entrance to the Mersey has increased to about 0.9 m, there is little or no surge elevation in the region close to location D. In essence, the surge continues to propagate farther up the estuary at this time rather than to flood this shallow region. The storm surge propagation into the estuary at this time (namely 2300 hours, 11 November) is clearly evident in the current vectors that show [Fig. 6d, (iii)] water entering the Mersey. However, in the region to the east of  $-2.85$  West [Fig. 6d, (iii)], where water level had previously increased, there is a flow to the west. This flow together with that entering the Mersey is responsible for the build-up of elevation in the Liverpool region and the maximum surge that occurred at 0100 hours 12 November (Fig. 4b). However, the increased surge elevation in Liverpool Bay in essence floods the near-shore region at the top of the Wirral Peninsular (location A) [Fig. 6d, (ii)], thereby removing the spatial variability found previously [Fig. 6c, (ii)].

From 2300 hours 11 November to 0000 hours 12 November, surge levels within the eastern Irish Sea, the Mersey and at Liverpool continue to rise, with the surge maximum propagating as far east as position W [Fig. 6e, (i) and (ii)]. At this time, the shallow water region at location C has been flooded by the surge. The surge reaches a maximum of about 1.4 m at about location W [Fig. 6e, (ii)] in the upper reaches of the Mersey. At this position, there is a narrow across estuary bar (Fig. 3b), which inhibits surge propagation further into the estuary.

Over the next hour (from 0000 to 0100 hours, 12 November), surge elevations at D and V decrease [Fig. 6f, (i) and (ii)], with surge elevations at Liverpool (position L) reaching a maximum [Figs. 4b and 6f, (i)]. Subsequently, as surge elevations at the entrance to the Mersey decrease, there is a flow out of the Mersey near its entrance [Fig. 6f, (iii)]. However, further down the Mersey, there is a flow to the west causing elevations to rise near its head. In essence, although surge elevations decrease in the region of locations V and W [compare Fig. 6e (ii) and f (ii)], the surge continues to propagate farther up the Mersey giving rise to a maximum of over 2 m near location X [Fig. 6f, (ii)]. The up-estuary flow in the shallow water away from the Mersey entrance [Fig. 6f, (iii)], is associated with direct wind forced currents in these shallow regions at a time of near maximum wind stress in the region (Fig. 4a). Although direct wind forced flow in shallow water does not move a large volume of water



(due to the shallow nature of the region) and hence generate large surges, it does produce appreciable currents.

Subsequently (namely from 0100 to 0200 hours, 12 November) as water levels within the Mersey decrease [compare Fig. 6f (i) and (ii) and g (i) and (ii)], there is a reduction in the surge in the region of locations V. However, the presence of the across channel bar near location W prevents the flow from the region of positive surge to the west of this back into the main body of the Mersey. Consequently, the surge elevation remains unchanged in the “pools” that occur between locations W and X [compare Fig. 6f (ii) and g (ii)]. Over the next hour (from 0200 to 0300 hours, 12 November), as surge elevations decrease in Liverpool Bay and over the whole Irish Sea, surge elevations in the Mersey decrease (Fig. 6h) as water flows out of the region. As previously during the start of surge propagation into the Mersey, there is significant spatial variability in surge elevations in the region of Liverpool and particularly near locations A–D reflecting local variations in topography (Fig. 6h).

It is evident from Fig. 6h that, although the surge elevation has significantly reduced over the majority of the Mersey, the small area of positive surge remains in its upper reaches between locations W and X. As previously, an expanded plot of Fig. 6h in its upper reaches (not presented) shows that this region lies between the two areas where the across channel topography is above MSL (Fig. 3b). As discussed previously in connection with Fig. 3b, water depths below MSL are denoted by negative values, with positive values denoting those above MSL. Consequently, when the model starts from a state of rest, these areas of positive water depth are dry. As the tide and surge propagate down the Mersey, these regions become wet as water passes over them. However, when the flow reverses, water flows over them until they become dry when flow ceases. At this time, water in deeper upstream regions is trapped. This gives rise to a positive elevation up to a maximum of the value of the positive water depth, as seen here.

Over the next 3 h, as wind stresses over the Irish Sea decrease, water levels within the Mersey (not presented) show a reduction in surge elevation. Associated with this are complex spatial variations in surge elevation reflecting the water depth variations within the Mersey (Fig. 3a, b) and the influence of tide–surge interaction.

### 3.3 The negative surge of 1100 hours 13 November

Following the major positive surge over the Irish Sea at about 0000 hours 12 November, the magnitude of the westerly wind stress decreased, with the southerly wind

stress changing to one from the north (Fig. 4a). This led to a decrease in surge elevations over the sea region off the west coast of Britain, producing a negative surge on the 13 November as shown in Fig. 4b.

This negative surge was a maximum at 1100 hours 13 November giving surge elevations of about  $-0.3$  m over the whole eastern Irish Sea (not presented). Although the offshore distribution of this surge had been computed previously (DJ92) with finite difference models, its spatial variability in near coastal estuaries had never previously been considered due to the coarse grid nature of these models. In the present finite element model, since the mesh is sufficiently fine to resolve the near-shore regions, it is possible to examine the spatial variability of the surge at the entrance to the Mersey and within it.

It is evident from Fig. 6i that there is significant spatial variability in the negative surge propagation within the Mersey. As in the case of the positive surge, the negative surge is largest within the deep water channel within the estuary. Small regions of positive surge remain in areas close to locations C and D and higher up the estuary. However, as surge elevations progressively become more negative in Liverpool Bay, surge currents show an outflow from the Mersey and surge elevations within the estuary decrease except in the region between locations W and X for the reasons discussed previously. The high degree of spatial variability of surge elevations within the Mersey suggest that the location of the nodal point used to make comparisons with tide gauges or current metres will be critical. However, in order to compare the present results with those from an earlier finite difference calculation (DJ96), exactly the same points were used (Fig. 4b). From Fig. 4b, it is evident that both models (finite difference and the present finite element) give comparable time series of storm surge elevation. However, the present model in common with an earlier finite element model that did not resolve the Mersey (JD08) underestimates the surge peak at Liverpool. This may be due to the fact that both these models used the same depth distribution as DJ96 in order to make comparisons with that model. Hence, although the present model incorporates a high-resolution representation of the Mersey, it may be necessary to improve the accuracy and resolution in the Liverpool Bay region in order to increase the surge peak at Liverpool. However, since the main objective of the present paper was to examine storm surge variability within the Mersey, this has clearly been demonstrated using the accurate Mersey bathymetry incorporated into the present model. In previous calculations with a coarse grid or mesh representation of the Mersey, there was no indication of the complex spatial patterns seen here.

#### 4 Concluding discussion

An unstructured mesh model of the west coast of Britain used previously to examine tides (Jones and Davies 2005, 2007a) and tidal residuals (Jones and Davies 2007b) in the region has been applied to a study of the storm surge of 11–14 November 1977. Previous calculations examined the response to uniform orthogonal winds (JD06) with a subsequent study considering the large-scale propagation of the November 1977 surge in the sea region (JD08). In that study, although an irregular mesh was used, no account was taken of the Mersey estuary or details of the near-shore variability of the surge. In the present work, the mesh used in JD08 is extended to include a high-resolution representation of the Mersey estuary. Previous work using this model (Jones and Davies, manuscript under (moderate) revision) showed that it could accurately reproduce tides in the region and the complex distribution of tidal currents within the Mersey. The focus in the present paper is to use that high-resolution model to examine surge propagation in the Liverpool Bay region and the Mersey estuary.

Surge calculations showed that elevations over the eastern Irish Sea were comparable to those found previously using a limited area high-resolution finite difference model (JD96) or unstructured mesh model (JD08). In addition, storm surge elevations at eastern Irish Sea locations away from the Liverpool Bay area were not significantly different from those computed by JD08. However, in the region of Liverpool Bay, adjacent to the Mersey entrance and particularly within the Mersey, there were some differences in the solution. This suggests that including a more detailed model of the Mersey within a larger area model does influence the surge within the Liverpool Bay region adjacent to the Mersey. A detailed study of surge propagation within the Mersey showed that, as elevations increased within Liverpool Bay, the surge propagated down the Mersey. The speed of propagation of the surge and its amplitude were largest in the deep water channels, and hence, the spatial and temporal variability of the surge was appreciably influenced by bottom topography.

As the surge propagates from the entrance of the Mersey towards its head, surge amplitude increases as water depth and cross-channel area decrease. As winds over the Irish Sea decrease, water level at the entrance to the Mersey is reduced. However, in many cases, the surge continues to propagate up the Mersey estuary with surge elevation maximum increasing due to a reduction in water depth and narrowing of the estuary. Calculations show that, at some times, there appears to be a reflected wave from the upper reaches of the Mersey, which propagates towards its

entrance giving rise to a local increase in what would otherwise be a decreasing surge as it propagates towards the mouth of the Mersey. This complex behaviour of the surge in the Mersey estuary had not been previously appreciated due to the coarse grid nature of earlier models of the area. Some regions of trapped water are left in the upper reaches of the Mersey in areas that were flooded by the surge.

Calculations show that the wind field over the region of the model has a significant influence upon the spatial and temporal variability of surges in the eastern Irish Sea and Liverpool Bay. However, in terms of the dynamics of the surge elevation within the Mersey, the main control is topography and surge elevation at its entrance, with the local wind field having little effect. The local wind does however contribute to the intensity of the storm surge currents within the shallow regions of the Mersey. The shallow water nature of the region suggests that bottom frictional effects and additional friction due to wind waves (e.g. Jones and Davies 2001) will play a role, and calculations aimed at examining this are in progress. In addition, the use of higher resolution topography at the head of the Mersey river would allow small channels to be resolved that would influence surge “pooling” in this region, as would the inclusion of a river discharge that has been excluded here.

**Acknowledgements** The origin of the TELEMAC system is EDF-LNHE and is therefore ©EDF-LNHE. Thanks are due to Andrew Lane for providing accurate Mersey bathymetry. The authors are indebted to R.A. Smith for help in preparing figures and L. Parry and E. Ashton for typing the text.

#### References

- Bernier NB, Thompson KR (2006) Predicting the frequency of storm surges and extreme sea levels in the northwest Atlantic. *Journal of Geophysical Research*, 111, C100009. doi:10.1029/2005JC003168
- Bobanovic J, Thompson KR, Desjardins S, Ritchie H (2005) Forecasting storm surges along the east coast of Canada and the northeastern U.S.: the storm of 21 January 2000. *Atmos-Ocean* 44(2):151–161
- Davies AM, Jones JE (1992) A three-dimensional wind driven circulation model of the Celtic and Irish Seas. *Cont Shelf Res* 12:159–188
- Davies AM, Jones JE (1996) Sensitivity of tidal bed stress distributions, near bed currents, overtides and tidal residuals to frictional effects in the eastern Irish Sea. *J Phys Oceanogr* 26:2553–2575
- Davies AM, Hall P (2002) Numerical problems associated with coupling models in shelf edge regions. *Appl Math Model* 26:807–831
- Davies AM, Kwong SCM, Flather RA (1998) A three-dimensional model of wind-driven circulation on the shelf: application to the storm of January 1993. *Cont Shelf Res* 18:289–340

- Fernandes EHL, Dyer KR, Moller OO, Niencheski LFH (2002) The Patos lagoon hydrodynamics during an El Nino event (1998). *Cont Shelf Res* 22:1699–1713
- Fernandes EHL, Marino-Tapia I, Dyer KR, Moller OO (2004) The attenuation of tidal and subtidal oscillations in the Patos Lagoon estuary. *Ocean Dyn* 54:348–359
- Flather RA, Hubbert KP (1989) Tide and surge models for shallow water—Morecambe Bay revisited. In: Davies AM (ed) *Modeling marine systems*, vol 1. CRC, Boca Raton, pp 135–166
- Greenberg DA, Dupont F, Lyard FH, Lynch DR, Werner FE (2007) Resolution issues in numerical models of oceanic and coastal circulation. *Cont Shelf Res* 27:1317–1343
- Hagen S, Westerink J, Kolar R, Horstmann O (2001) Two dimensional unstructured mesh generation for tidal models. *Int J Numer Methods Fluids* 35:669–686
- Hagen SC, Horstmann O, Bennett RJ (2002) An unstructured mesh generation algorithm for shallow water modeling. *Int J Comput Fluid Dyn* 16(2):83–91
- Heaps NS (1983) Storm surges, 1967–1982. *Geophys J Roy Astron Soc* 74:331–376
- Horsburgh KJ, Wilson C (2007) Tide–surge interaction and its role in the distribution of surge residuals in the North Sea. *J Geophys Res* 112:C08003. doi:10.1029/2006JC004033
- Ip JTC, Lynch DR, Friedrichs CT (1998) Simulation of estuarine flooding and dewatering with application to Great Bay, New Hampshire. *Estuar Coast Shelf Sci* 47:119–141
- Jones JE (2002) Coastal and shelf-sea modelling in the European context. *Oceanogr Mar Biol Annu Rev* 40:37–141
- Jones JE, Davies AM (1998) Storm surge computations for the Irish Sea using a three-dimensional numerical model including wave–current interaction. *Cont Shelf Res* 18:201–251
- Jones JE, Davies AM (2001) Influence of wave–current interaction and high frequency forcing upon storm induced currents and elevations. *Estuar Coast Shelf Sci* 53:397–414
- Jones JE, Davies AM (2005) An intercomparison between finite difference and finite element (TELEMAC) approaches to modelling west coast of Britain tides. *Ocean Dyn* 55:178–198
- Jones JE, Davies AM (2006) Application of a finite element model (TELEMAC) to computing the wind induced response of the Irish Sea. *Cont Shelf Res* 26:1519–1541
- Jones JE, Davies AM (2007a) On the sensitivity of computed higher tidal harmonics to mesh size in a finite element model. *Cont Shelf Res* 27:1908–1927
- Jones JE, Davies AM (2007b) On the sensitivity of tidal residuals off the west coast of Britain to mesh resolution. *Cont Shelf Res* 27:64–81
- Jones JE, Davies AM (2008) Storm surge computations for the west coast of Britain using a finite element model (TELEMAC). *Ocean Dynamics* 58:337–363
- Lane A (2004) Bathymetric evolution of the Mersey Estuary, UK, 1906–1997: causes and effects. *Estuar Coast Shelf Sci* 59:249–263
- Legrand S, Deleersnijder E, Hanert E, Legat V, Wolanski E (2006) High-resolution, unstructured meshes for hydrodynamic models of the Great Barrier Reef, Australia. *Estuar Coast Shelf Sci* 68:36–46
- Legrand S, Deleersnijder E, Delhez E, Legat V (2007) Unstructured, anisotropic mesh generation for the Northwestern European continental shelf, the continental slope and the neighbouring ocean. *Cont Shelf Res* 27:1344–1356
- Levasseur A, Shi L, Wells NC, Purdie DA, Kelly-Gerrey BA (2007) A three-dimensional hydrodynamic model of estuarine circulation with an application to Southampton Water, U.K. *Estuar Coast Shelf Sci* 73:753–767
- Nicolle A, Karpytchev M (2007) Evidence for spatially variable friction from tidal amplification and asymmetry in the Pertuis Breton Bay of Biscay, France. *Cont Shelf Res* 27:2346–2356
- Walters RA (2005) Coastal ocean models: two useful finite element methods. *Cont Shelf Res* 25:775–793
- Werner FE (1995) A field test case for tidally forced flows: a review of the tidal flow forum. In: Lynch DR, Davies AM (eds) *Quantitative skill assessment for coastal ocean models*. American Geophysical Union, Washington, pp 269–284